





# Underwater Sound Emissions from the Moorings of Floating Wind Turbines: HYWIND Scotland Case Study

Federica Pace , Robin D. J. Burns, S. Bruce Martin , Michael A. Wood, Colleen C. Wilson, C. Eric Lumsden, Kari Mette Murvoll, and Jürgen Weissenberger

## Contents

Introduction .....	2
Sound from Operational OWTs .....	3
Acoustic Data Collection .....	5
Recording Specifications .....	5
Acoustic Data Analysis .....	5
Kurtosis Estimation .....	8
Acoustic Modeling .....	8
HS-2 Source Levels Estimation .....	9
Results .....	9
Impulsiveness Analysis .....	14
Marine Mammal Impact Modeling .....	18
Conclusions .....	19
References .....	22

Parts of this chapter have been reproduced with permission from the following source: Burns et al. (HYWIND Scotland floating offshore wind farm: sound source characterisation of operational floating turbines. Document number 02521, version 2.0. Technical report by JASCO Applied Sciences for Equinor Energy AS, 2022).

F. Pace (✉)

JASCO Applied Sciences, Schwentinental, Germany

e-mail: [federica.pace@jasco.com](mailto:federica.pace@jasco.com)

R. D. J. Burns · M. A. Wood

JASCO Applied Sciences, Hampshire, UK

e-mail: [robin.burns@jasco.com](mailto:robin.burns@jasco.com); [michael.wood@jasco.com](mailto:michael.wood@jasco.com)

S. B. Martin · C. C. Wilson · C. E. Lumsden

JASCO Applied Sciences, Halifax, Canada

e-mail: [bruce.martin@jasco.com](mailto:bruce.martin@jasco.com); [colleen.wilson@jasco.com](mailto:colleen.wilson@jasco.com); [eric.lumsden@jasco.com](mailto:eric.lumsden@jasco.com)

K. M. Murvoll · J. Weissenberger

Equinor ASA, Herøya Forskningspark, Norway

e-mail: [kmmu@equinor.com](mailto:kmmu@equinor.com); [jurw@equinor.com](mailto:jurw@equinor.com)

© Springer Nature Switzerland AG 2024

A. N. Popper et al. (eds.), *The Effects of Noise on Aquatic Life*,

[https://doi.org/10.1007/978-3-031-10417-6\\_121-1](https://doi.org/10.1007/978-3-031-10417-6_121-1)

---

**Abstract**

The nature of underwater sound generated by floating offshore wind turbines (OWTs) is of increasing interest to the renewable energy industry. This chapter presents the findings from the measurements of the first operational floating OWF, HYWIND Scotland.

Two acoustic recorders were deployed for 4 months: one at a control site and one within the OWF. Continuous tonal sounds associated with the turbine operations and transient sounds originating from the moorings were identified. The characteristics of the latter and the relevant implications for impact assessment are described. A kurtosis analysis of the sounds from the moorings of the HYWIND turbines indicated that the signals were more non-impulsive than impulsive. Directional analysis of the acoustic data revealed that different types of sounds (i.e., creaks, snaps, rattles) were generated from each of the three monitored turbines despite these having the same design. The loudness of their signals also varied according to the source. These findings show the importance of collecting in-field measurements to inform impact assessment studies. Due to the variability of these signals, characteristics from mooring noise are difficult to predict in underwater noise modeling studies.

---

**Keywords**

Sound · Offshore wind · Impact · Operational · Floating · Wind turbine · Kurtosis

---

**Introduction**

Understanding the nature of underwater sound from floating offshore wind turbines (OWTs) is a topic of increasing interest in the renewable energy industry. There are ambitious plans to develop large floating offshore wind farms (OWFs) around the world. OWFs up to 54 GW are currently proposed for construction. Each will be required to submit detailed impact assessment studies that estimate the effects of sound on marine life, among other effects.

Sound emissions from fixed-structure OWTs, such as monopiles, have been extensively measured and evaluated during installation and operation. Fixed-structure OWTs are appropriate for water depths up to ~60 m; however, in deeper locations, other approaches are planned, with a leading design being floating foundations secured to the seabed with mooring lines. No public literature is available on measurements from floating foundations because only a few have been installed to date.

HYWIND Scotland is the world's first operational floating OWF and comprises five wind turbine generators (WTGs) for a total installed capacity of 30 MW. Each WTG is mounted on a spar buoy/pillar moored to the seabed by a ballasted catenary system employing three mooring cables (Fig. 1).

**Fig. 1** Diagram of the HYWIND Scotland WTG. (Source: Equinor ASA)



JASCO conducted a sound source characterization (SSC) study for Equinor (previously Statoil) in 2011 on a similar mooring system deployed as part of the HYWIND DEMO system off the coast of Stavanger, Norway. Those measurements led to the identification of tonal and transient sounds (e.g., snapping and clicking) generated by the turbine; the latter may be associated with the mooring system (Martin et al. 2011).

The focus of this chapter is to present an operational noise profile for the HYWIND Scotland system, describing the characteristics of the sound signals associated with the moorings of these systems and discussing the implications for their impact on marine fauna.

## Sound from Operational OWTs

Underwater sound from any type of wind turbine in operation originates in the moving mechanical parts in the nacelle, almost exclusively with energy emitted at low frequencies below 1 kHz and typically with strong tonal elements at the frequencies corresponding to the rotation of the gears and their harmonics (Pangerc

et al. 2016). Noise is transmitted through the tower and radiates into the water from the submerged section. The underwater operational sound levels might therefore depend on the type of foundation, but this has not been demonstrated by the studies conducted to date (Tougaard et al. 2020). Two factors that influence the sound level are the turbine size and the wind strength. As the size of blades increases, the mechanical forces acting on the gears and bearings also increase, resulting in higher noise levels; the same is true for an increase in wind speed (Tougaard et al. 2020). The underwater sound levels emitted by operational turbines have the potential to impact marine fauna, particularly when considering the sound fields generated by several turbines within a wind farm (Stöber and Thomsen 2021).

With regard to floating WTGs, additional potential sources of underwater sound have been identified (Martin et al. 2011). These include the mooring systems and equipment that may be project specific (this may vary according to the float solution chosen), such as pumps that may be used to ballast semi-submersible platforms. As these elements are project specific, predicting their sound signature and associated levels may be difficult to predict, especially in the environmental impact assessments when the detailed design may not have been defined. For this reason, collecting in-field measurements to characterize the signals emitted by the WTGs once installed as full-scale systems is useful.

Sound emissions associated with ballasting pumps are expected to be of a continuous nature, given that they use the same type of propellers as ballasting ships. These will also generate low-frequency tones according to their dimensions and rotational speed specifications; however, little literature is available that studied this specific component as it is not a ship's main source of underwater radiated noise (URN). Nevertheless, the pumps are activated when the wind changes directions; therefore, depending on the volume of water to be transferred, they are active for a few minutes when such an event occurs, rather than pumping constantly.

The sound emissions from the moorings of floating turbines are comparable to chains and catenaries regularly used for offshore moorings, for instance, for ocean buoys collecting long-term data. While it is common knowledge that such moorings generate sound as they move vertically and horizontally in the water column with the movement of waves, current, and tide, their signature has not been described in the literature. Typically, this source is referred to in the available literature as an "undesired" source because studies are dedicated to characterizing anthropogenic activities and mooring noise is not the target of the investigation. Moorings on buoys dedicated to acoustic monitoring are therefore designed to be as quiet as possible to ensure that this source does not impact the quality of the data by masking the target source(s) or clipping the recordings (Robinson et al. 2014). Sounds from moorings are transient, but they can occur very regularly throughout a mooring's deployment. Therefore, characterizing and assessing the potential impacts of these elements requires further investigation. Transient noises (at ~23 second intervals) with  $L_{0-p}$  greater than 160 dB re 1  $\mu$ Pa likely related to tension releases in the moorings from floating WTGs were described for the HYWIND demo project (Martin et al. 2011), which was a single, small-scale, floating turbine installed offshore of Norway.

## Acoustic Data Collection

All underwater sound data was measured using JASCO's Autonomous Multichannel Acoustic Recorders (AMARs). One recorder (an AMAR G4) was positioned in the west-northwest area of the HYWIND site (Fig. 3). This recorder was 642 m from the turbine HS-1.

A second recorder (an AMAR G3 with a single omnidirectional hydrophone) was deployed approximately 13 km from the HYWIND site to collect "control" data for ambient sound.

## Recording Specifications

Both AMARs were fitted with GeoSpectrum Technologies Inc.'s omni-directional hydrophones (i.e., M36-V35-100 with a nominal sensitivity of  $-165$  dBV/ $\mu$ Pa with pre-amplification). Flow noise minimization was achieved by using an acoustically transparent shroud around the hydrophone cade.

The four hydrophones of the HYWIND mooring were mounted in an orthogonal arrangement with a nominal 50 cm spacing to allow the time of arrivals from different directions to be determined (Fig. 2). Precise measurements of the relative distance between hydrophones were taken and used as inputs for the directional calculations.

The AMARs recorded continuously at a 64,000 Hz sample rate to return a recorded bandwidth of 10–32,000 Hz. The recording channels had a 24-bit resolution with a spectral noise floor of 32 dB re 1  $\mu$ Pa<sup>2</sup>/Hz and a nominal ceiling of 165 dB re 1  $\mu$ Pa. Acoustic data were stored on 13  $\times$  512 GB flash memory cards for each instrument. JASCO field staff calibrated the AMARs before deploying and after retrieving them. Calibrations were performed using a pistonphone type 42 AC precision sound source (G.R.A.S. Sound & Vibration A/S). At both sites, the AMARs logged data 24 h per day from 21 October 2020 to 24 January 2021 (Table 1). Approximately 6.6 TB of data were collected.

## Acoustic Data Analysis

The acoustic analysis methods and the terminology used were in accordance with ISO 18,405:2017 (ISO 2017).

The bearing angles of each hydrophone were calculated based on their relative distances and positions with respect to each wind turbine (Table 2). The correct orientation of the array was further confirmed by correlating the bearings obtained from the analysis of the signature of the vessel used for deploying and retrieving the recorders, *SWATH 1* with actual bearings calculated from the positions of the vessel's GPS track log.

The orthogonal hydrophone array allowed for the spatial discrimination of bearing and elevation of detected sound. Such data was stored for individual events

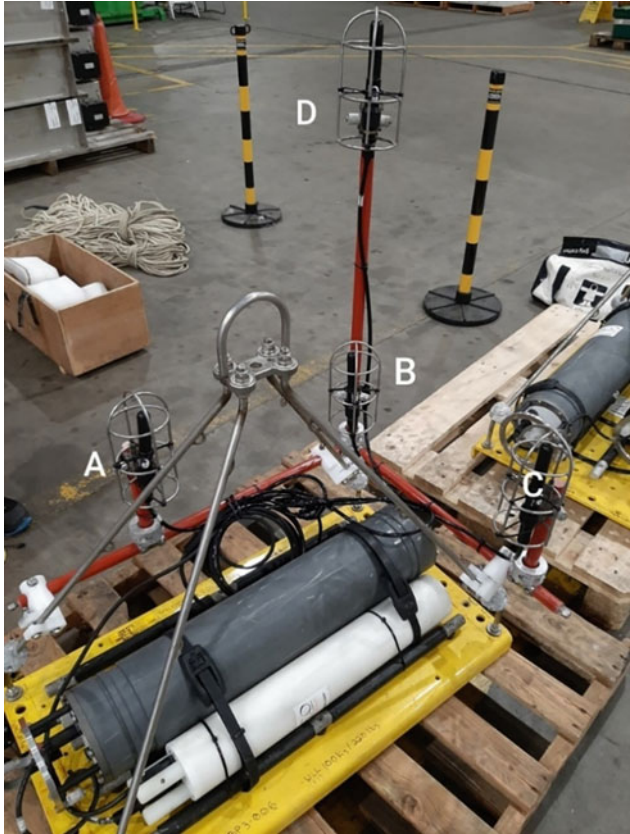


**Fig. 2** Photo of the HYWIND equipment before it was deployed. The assembly includes an AMAR G4 (white tube) fixed on a baseplate, a battery back (gray tube), and the four hydrophones mounted on a fiberglass frame (red tubes)

for later analysis. The bearing to each time/frequency cell is color coded and displayed using directograms (Fig. 3); this type of image shows the direction of a sound source relative to the array. The radial resolution obtained was 22.5 degrees. The color wheel represents sound originating from different directions. For instance, sound propagating from the north of the AMAR would be presented in a shade of red, while from the south would be colored in light blue.

Impulses were detected using a Teager-Kaiser energy detector (Kaiser 1990, Kandia and Stylianou 2006). Two distinct tonal continuous sounds below 100 Hz were identified during the analysis; these were identified as part of the floating turbines' signature. Both tones would affect the performance of the impulse detector and were therefore filtered out of the transient signals analysis. For the latter, a high-pass filter was applied (stop band  $f = 85$  Hz, passband  $f = 100$  Hz). A 100 ms energy time series was obtained by filtering the squared time series, then summing over a 100 ms window, and then dividing by the number of samples in the window. The

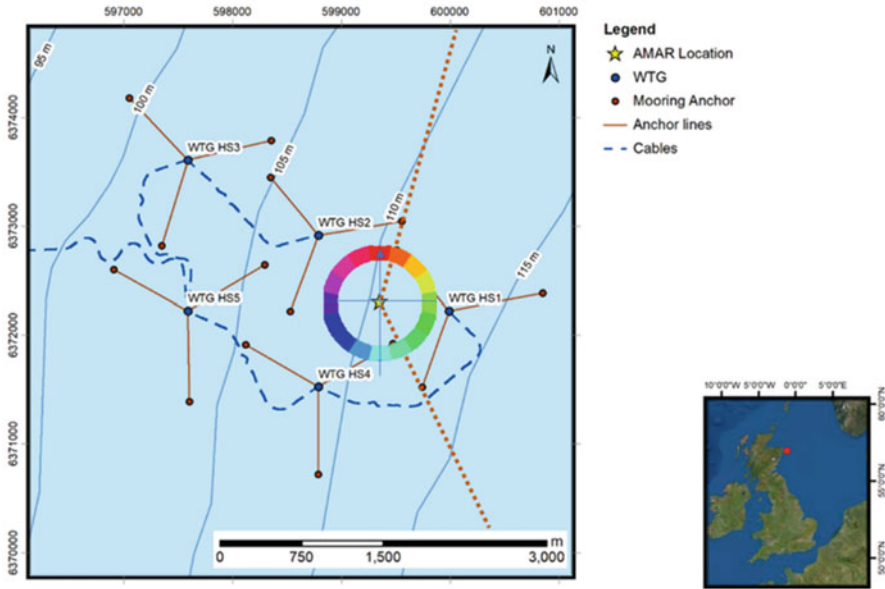


**Fig. 3** Map showing the layout of the wind turbines. The color wheel is oriented relative to north

**Table 1** Dates and locations the two AMARs deployed (UTM 30 N, WGS84). Retrieval times (UTC) indicate the time when each retrieval started

Location	Deployment	Retrieval	Latitude	Longitude	Easting	Northing	Water depth (m)
HYWIND	21 Oct 202013:44	15 Jul 2021 10.30	57° 29.109' N	001° 20.571' E	599348.894	6372604.308	112
Control	21 Oct 202011:43	24 Jan 2021 13:05	57° 31.801' N	001° 07.580' E	612189.991	6377935.635	95

**Table 2** Distances and bearings of each HYWIND WTG from the AMAR deployed within the Hywind Scotland OWF from Burns et al. (2022)

WTG	Distance (m)	Bearing (°)
HS-1	605	095
HS-2	880	318
HS-3	2242	308
HS-4	951	1799
HS-5	1799	269

time series was divided by its mean value for each 20-s long data buffer that was passed to the Teager-Kaiser operator (Kaiser 1990, Kandia and Stylianos 2006). Normalizing this buffer by its mean value allowed for the use of a fixed threshold that was independent of the absolute magnitude of the raw time-series data. A detection threshold of 15 was chosen for the Teager-Kaiser operator. The detector



was set with a 1.0 s “lock-out” after each strike was detected; this minimized false alarms on multipath arrivals.

## Kurtosis Estimation

Understanding whether signals are impulsive or non-impulsive is important when selecting which hearing threshold shift regulatory criteria to apply (NMFS 2018). In recent years, kurtosis has been suggested as an objective metric to determine the impulsiveness of a sound source (Martin et al. 2020, Müller et al. 2020). Kurtosis was therefore calculated for the evaluation of the broadband transient signals identified in the recordings to determine the most appropriate applicable criteria for impact assessment.

Kurtosis ( $\beta$ ) is defined as the ratio of the fourth moment to the squared second moment of the instantaneous sound pressure:

$$\beta = \frac{\frac{1}{N} \sum (p_i - \bar{p})^4}{\left[ \frac{1}{N} \sum (p_i - \bar{p})^2 \right]^2} \quad (1)$$

where the  $i$ th sample of the instantaneous sound pressure is  $p_i$ , the sound pressure’s arithmetic mean is  $\bar{p}$ , and the number of data samples in the analysis window that affects the resulting value for kurtosis is  $N$ . As Martin et al. (2020) suggest, this project applied a 60 s analysis window. A kurtosis value of 3 represents random Gaussian noise. When deciding if a soundscape is impulsive to help determine whether an impulsive or non-impulsive hearing threshold shift threshold is exceeded, kurtosis value of 40 is used as the threshold (NFMS 2018). A kurtosis value of approximately 3 also represents wind-driven underwater ambient sound.

## Acoustic Modeling

Sound propagation modeling was performed for two purposes: to compute the source level of the sounds emitted from the turbines (i.e., back-propagation) and then to forward propagate the source levels to determine sound levels as a function of distances from the turbines. The modeling assumed that a point source could represent the turbine spar (cylinder shaped). The reported nominal draft of the spar was 78 m, with the point source being modeled at the mid-point (i.e., source depth of 39 m).

JASCO’s Marine Operations Noise Model (MONM)(Austin and Chapman 2011), which is based on the parabolic equation (Collins 1998), was used for low-frequency propagation (less than 1 kHz) combined with BELLHOP for frequencies above 1 kHz.

Decade bands in the range 10 Hz–25 kHz were modeled. The algorithm developed by Harrison and Harrison (1995) was used to consider sounds across each



frequency band (as opposed to individual frequencies). This algorithm uses a range-dependent smoothing factor to simulate a frequency smearing in frequency, eliminating peaks and troughs in the sound field.

## HS-2 Source Levels Estimation

Source levels ( $L_s$ ) were estimated for a single turbine (i.e., HS-2, the dominant in terms of received levels among the three turbines) according to:

$$L_s = L_p + N_{PL}. \quad (2)$$

where  $L_s$  is the source level,  $L_p$  is the sound pressure level (1 min), and  $N_{PL}$  is the propagation loss, as per (ISO 2017) terminology.

It is only possible to back-propagate the sound levels recorded at the HYWIND monitoring station. As such, the full frequency spectra from 10 Hz to 25 kHz were included. In the low frequencies (i.e., below 100 Hz), the sound signature of the wind turbine also included the tonal components (peaking around 24 and 75 Hz) that are associated with the electrical power generation and other unknown mechanical sources within the turbines. These are not described in detail in this publication.

The source levels presented may be overestimated when the difference in sound levels between the Control and Hywind Scotland sites at specific frequency bands is small. This is because the ambient sound in that frequency band would be back-propagated.

Figure 4 shows the propagation loss ( $N_{PL}$ ) calculated

The source levels calculated for the turbines at the different wind speeds are shown in Fig. 5 for the median (50th percentile) sound levels and Fig. 6 for the 5th percentile sound levels. For each analyzed wind speed, Table 3 shows the broadband back-propagated source levels in the 5th, 25th, 50th, 75th, and 5th percentiles.

There was a trend of increased sound levels with increased wind speed, as well as changes in the spectral characteristics. Noticeable peaks appeared at 20–25 Hz, 40 Hz, and 63–80 Hz and also at 1.0–1.25 kHz, especially at 20 knots and with the addition of a peak at 200–250 Hz at 25 knots (Burns et al. 2022).

---

## Results

Analyzing the acoustic data revealed a substantial amount of mooring noise. Several energy peaks were observed between 100 and 400 Hz. These appear to be associated with the regular transient sounds of the HYWIND mooring system components. The sounds are described as “snaps,” “creaks,” and “rattles.” These generally broadband transients occur irregularly, and their duration also varied, with typical durations between 0.2 and 1.0 s.

The transient sounds from the moorings are broadband, repetitive, and considerably less impulsive. These sounds are three types, described as “bangs,” “creaks,”

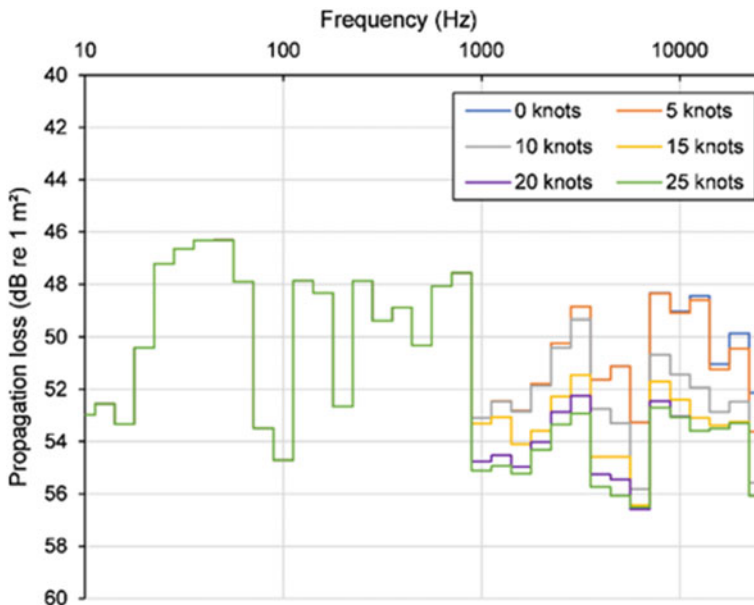


**Fig. 4** Propagation loss between the point source midway down the spar and the HYWIND recorder (880 m distance) for varying wind conditions. The propagation loss for bands below 1 kHz was calculated using the parabolic equation model that does not account for sea surface roughness (i.e., variation with wind speed). (©JASCO Applied Sciences)

and “rattles” during aural analysis. Aural analysis reveals that an action of tension release occurs in many of these noises. The rapid onset combined with the significant intensity of the sound visible in the spectrograms supports this.

In a 20-min segment recorded on 1 January 2021, human analysts manually annotated over 300 detections (Fig. 7). The audible broadband mooring transients shown on the directogram in Fig. 7 are consistently colored blue, pink, or green. This indicates that there were three, discrete, separate sources. The directions of HS-1 (eastward), HS-4 (south-westward), and HS-2 (north-westward) correspond exactly to the direction of the blue, pink, and green sectors on the color wheel. HS-1 and HS-4 are clearly generating less mooring noise than HS-2.

The transients originating from relatively small bearing clusters, aligned with HS-1, HS-2, and HS-4, were each acoustically different and distinct. There were also similar sound pressure levels for each cluster, which indicates a consistent source generation and distance (Figs. 8, 9, 10, and 11). The same type of mooring movement, such as surfaces rubbing under tension, appears to be generating the sounds. Most transient sounds are a repetition of staccato sounds; however, this mooring noise appears to have unique spectral and temporal identities for each turbine.

The low-frequency “bang” sound (green in Fig. 8) was associated with HS-1. The quietest of the three sounds, the bang was dominated by the lowest frequencies (<250 Hz). While these bangs were usually the shortest-duration sounds, they could,

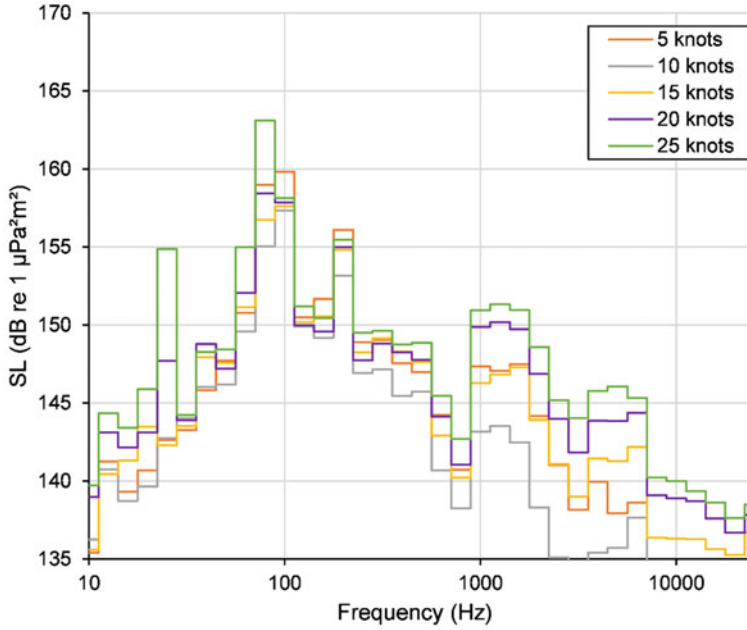


**Fig. 5** Median source levels calculated for turbine HS-1 at different wind speeds

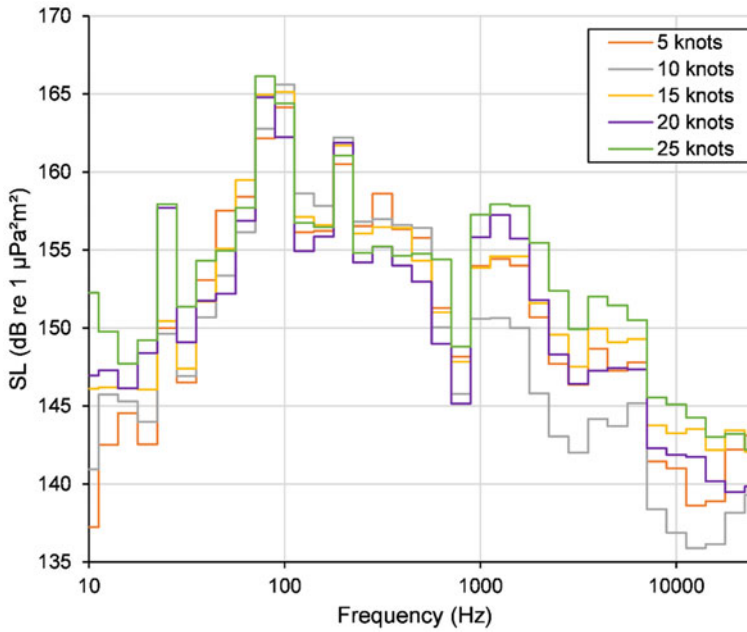


**Fig. 6** 95th percentile source levels calculated for turbine HS-1 at different wind speeds

**Table 3** Back-propagated broadband source levels (unit: dB re 1  $\mu\text{Pa}^2\text{m}^2$ ) for the 5th, 25th, 50th, 75th, and 95th percentiles

Wind speed (kn)	Broadband source level				
	5th percentile	25th percentile	Median percentile	75th percentile	95th percentile
5	158.9	161.5	165.1	167.2	170.5
10	156.7	160.1	162.5	165.6	170.8
15	159.6	162.0	163.9	166.5	171.4
20	160.4	162.8	164.8	167.2	170.6
25	162.1	164.9	167.2	169.3	172.0

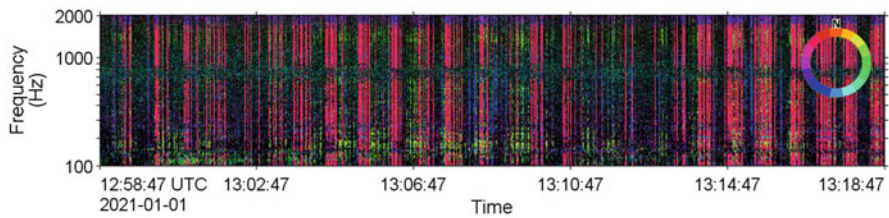


**Fig. 7** Directogram of 20 min of data during winds greater than 20 knots on 1 January 2021

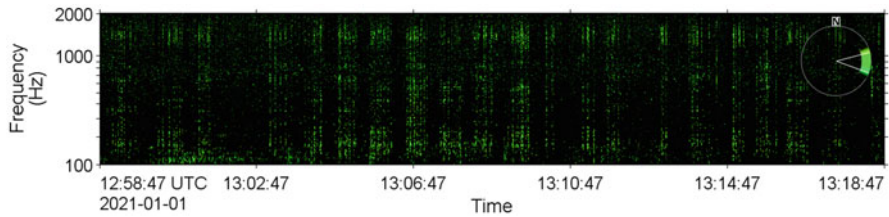


**Fig. 8** Directogram showing only transients received from the direction of HS-1

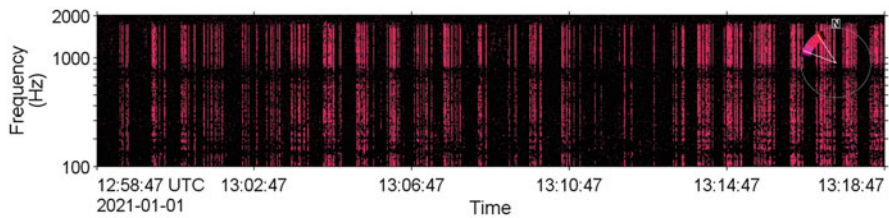


**Fig. 9** Directogram showing only transients received from the direction of HS-2

however, last for more than 2.5 s, with occasional instances of prolonged reverberation. This bang was not always audible because of masking by other sounds (or potentially by other ambient sounds).

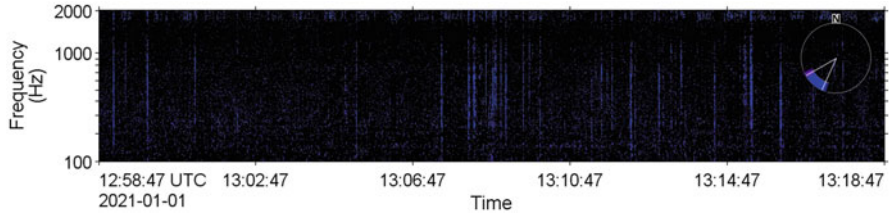


**Fig. 10** Directogram showing only transients received from HS-4 turbine

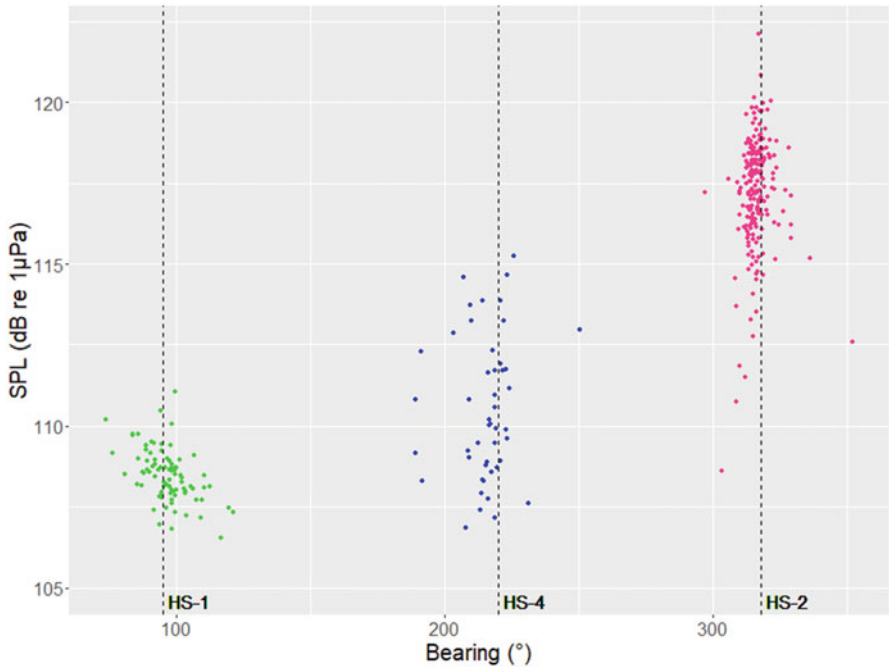


**Fig. 11** Plot of the transient bearing from the AMAR against sound pressure level (SPL) for 20 min on 1 January 2021. HS-1 “bang” transients (green), HS-2 “creak” transients (pink), and HS-4 “rattle” transients (blue). (Burns et al. 2022).

HS-2 generated a “creak” transient (red in Fig. 9). This had the highest SPL and masked the other two sounds when their occurrence overlapped. The duration of individual sounds was around 0.4 s, with some up to 1.5 s. This sound often had frequencies absent from the 700–900 Hz band.

HS-4 was associated with a “rattle” type sound (blue in Fig. 10). The duration of individual events varied from approximately 0.5 to 1.0 s. It sounded like a repeated tapping noise, with variable numbers of taps. The blue sounds had most of their energy in the 200–800 Hz band.

The variability in bearings versus received SPL for each transient sound type is presented in Fig. 11; this shows that the mooring noise levels differed for each HYWIND turbine and that the sound originated close to the bearing of the pillars. This indicates that the noise was restricted to the mooring components close to or at the pillar, rather than along the mooring chains. It is unclear why one mooring might be noisier than another when both experience the similar dynamic stresses.

The occurrence of mooring transients showed a positive correlation with wind speed but that was non-statistically significant. At higher wind speeds, the amount of mooring noise increased and substantially contributed to the wind farm's overall noise signature.

There was a stronger correlation between the occurrence of transient sounds and significant wave heights. This positive correlation may be due to a greater influence of waves, rather than wind speed, in causing the structure to heave, which therefore caused the mooring system to heave more.

The different transient sounds caused by the mooring were not mutually exclusive, and the data commonly showed combinations of different types of noise. This finding is consistent with the discovery that each HYWIND system seems to produce a unique type of mooring noise.

## Impulsiveness Analysis

A qualitative assessment of the impulses indicated that they tended to be on the order of 1 s long (Ainslie et al. 2021) and that multiple sub-pulses and/or tones were presented within the pulse. The pulses' peak pressures and rise times are clearly identifiable from the background but not as much as usual pile driving or seismic airgun impulses.

The detected impulses had interquartile durations of 1.3–1.7 s, which is longer than the conventional way an “impulse” is defined. As expected, a greater number of impulse detections at higher wind speeds at HYWIND were found by the detector; this was not replicated at the Control site (Fig. 12). As expected, the number of impulse detections at HYWIND decreased with increasing wind speed; above 100 Hz more wind-driven noise is present, which made detecting the impulses a more difficult task. One output of the impulse detector is the per-impulse sound exposure level in decidecade bands, and in Fig. 13 the mean, median, and 90th percentile of these are shown. Figure 14 shows auditory frequency weightings from the NMFS (2018) were applied to the decidecade SEL to determine the daily SEL. The impulsive SEL weighted high-frequency cetaceans were mostly 6 dB below the total daily SEL as shown Fig. 15, and they were commonly more than 10 dB below the total. The observation that there were more impulses at the HYWIND site (e.g., Fig. 12) is supported by comparing the kurtosis at HYWIND and the Control site, as shown in Fig. 16. However, highly impulsive minutes ( $\beta > 40$ ) were exceptionally rare at both HYWIND and the Control site. This kind of kurtosis distribution from a sound source is an excellent example of how applying a kurtosis-weighted SEL to predict hearing threshold shifts is valuable for regulatory applications (Zhao et al. 2010, see ► [“Impulsive or Non-Impulsive: Determining Hearing Loss Thresholds for Marine Mammals”](#) in the chapter by Zeddies et al., this volume).

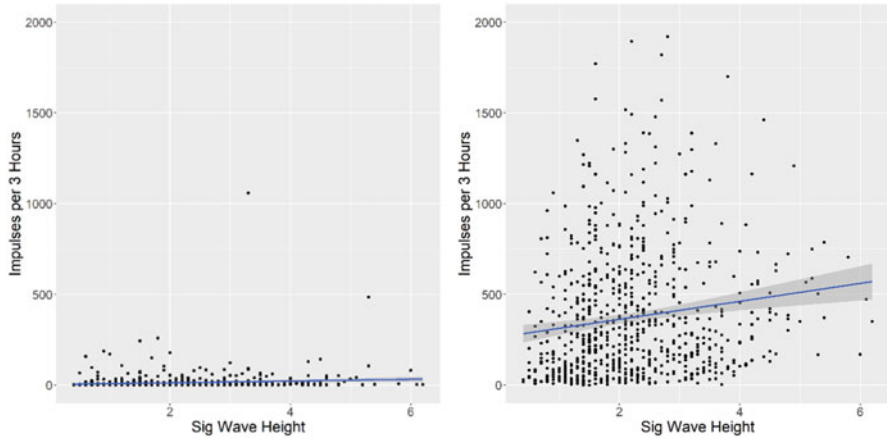


**Fig. 12** Scatterplot of the number of impulse detections per 3 h versus the significant wave heights at (left) the Control site and (right) HYWIND. (Burns et al. 2022)

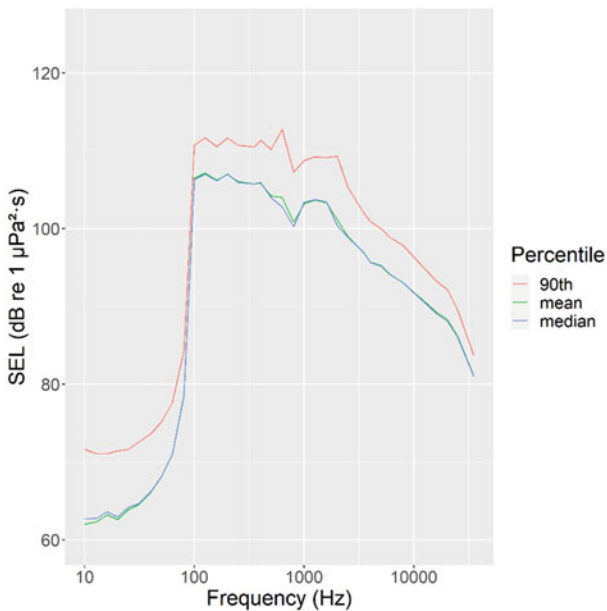


**Fig. 13** The decade sound exposure levels (SEL) of the impulses detected at HYWIND in the mean, median, and 90th percentile compared with the decade center frequencies

Use of the non-impulsive threshold from NMFS (2018) is recommended because minutes with a high kurtosis occurred relatively infrequently, the length of the impulses, and the impulsive SEL being 6 dB or higher below the total SEL. That is, the Temporary Threshold Shift (TTS) for high-frequency cetaceans (porpoise) would be 153 dB re 1  $\mu\text{Pa}^2\text{s}$ .



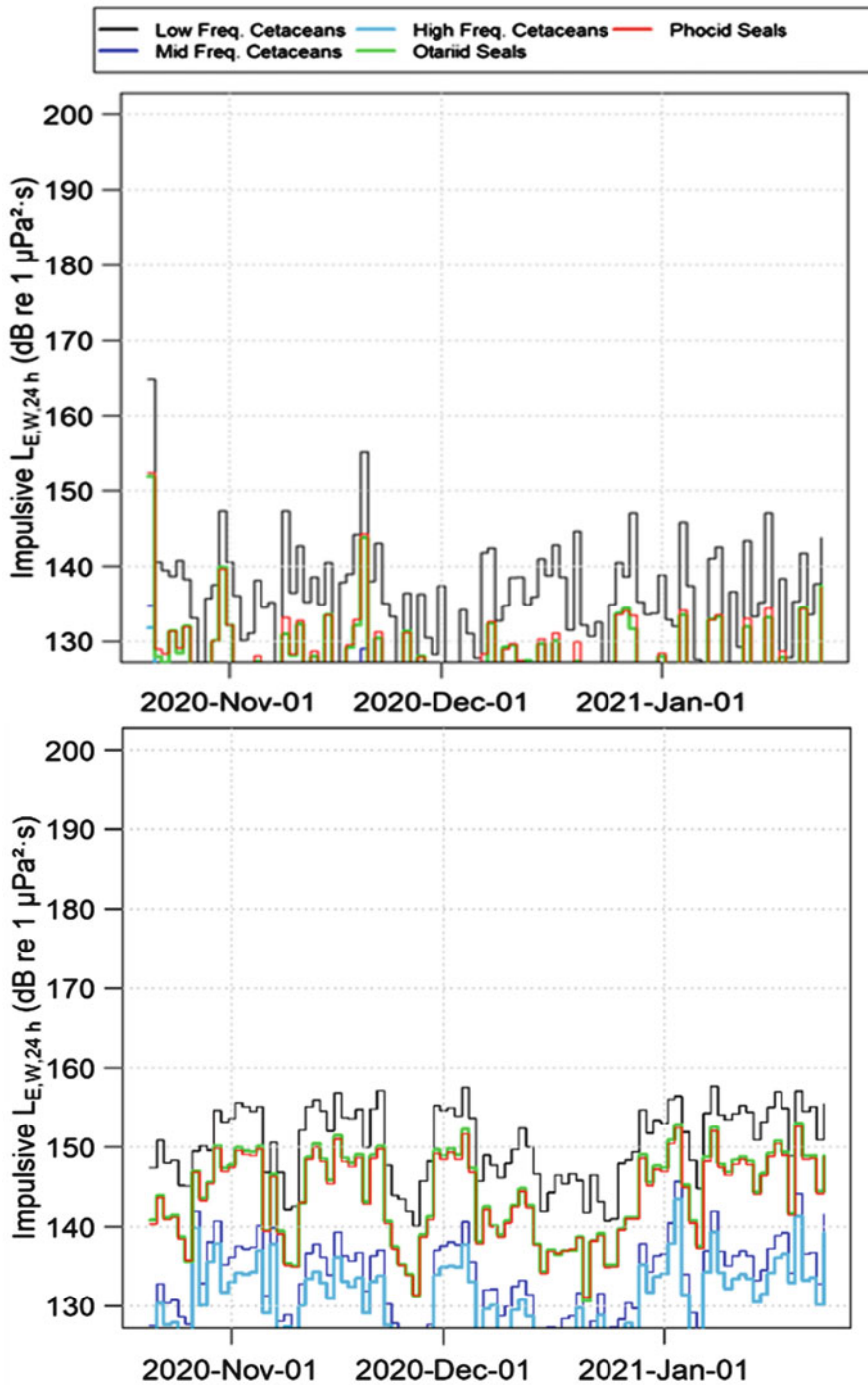


**Fig. 14** Daily auditory frequency weighted sound exposure level (SEL) for the transient events detected at (top) the Control site and (bottom) HYWIND

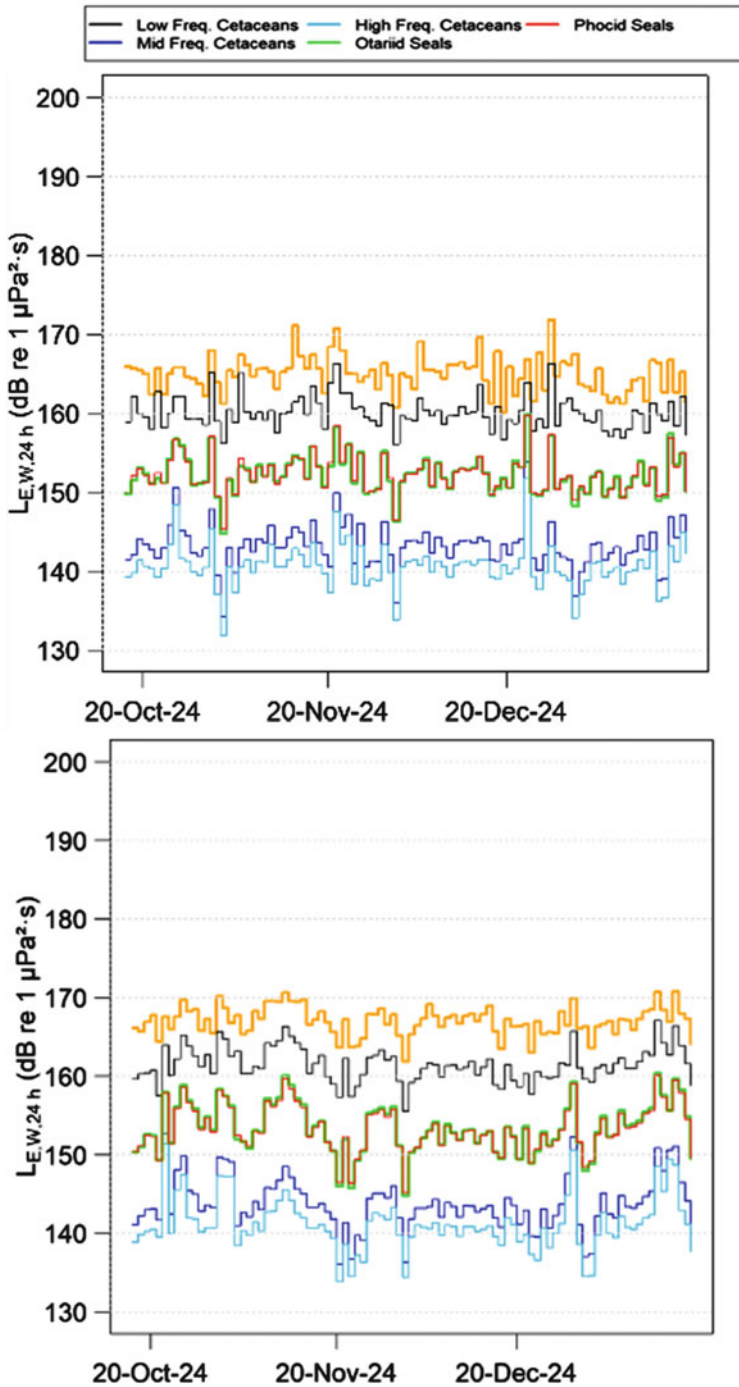


**Fig. 15** Daily auditory frequency weighted sound exposure level (SEL) for full days at (top) the Control site and (bottom) HYWIND

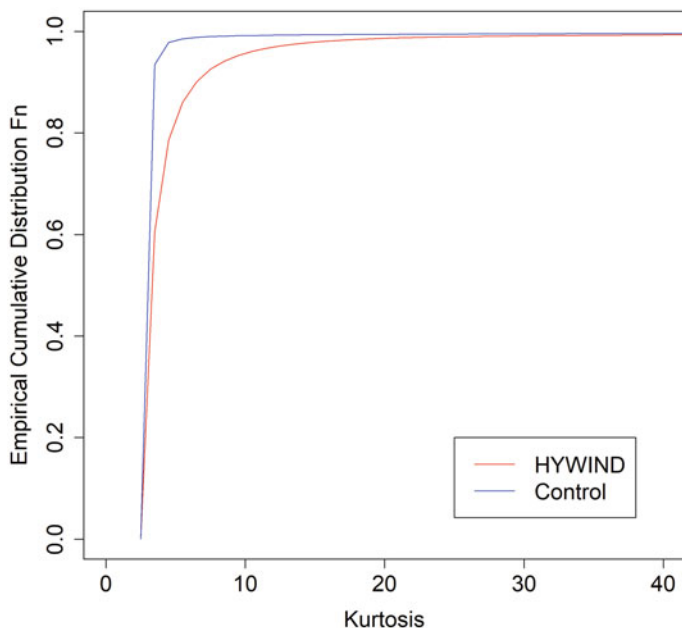


**Fig. 16** Empirical cumulative distribution functions for the 1-min kurtosis at the Control and HYWIND sites

## Marine Mammal Impact Modeling

Marine mammal impact modeling was performed using the same methods as the back-propagation; however, individual point sources representing the five turbines were modeled over  $360^\circ$  of radial transects. This provided a full three-dimensional (3-D) sound field. Maps of sound fields indicate the areas exposed to sound at certain levels. Figures 17 and 18 show examples representing the SPL for the 10-knot 50th-percentile and the 25-knot 95th-percentile sound fields, respectively.

The predicted levels for given conditions over the wider area, as well as the Southall et al. (2019) recommended maximum distances to impact thresholds, can be estimated by the model. In Table 4, the modeled weighted received SEL over 24 h for the considered auditory groups are shown, again presuming a constant windspeed of 15 knots, for the median and 75th percentile cases. In Table 5, the maximum modeled distances from the nearest turbine to the calculated isopleths associated with auditory impacts are shown, assuming a 24-h exposure at a 15-knot wind speed and taking the median and 75th percentile cases (i.e., sound levels that are constant over a 24 h).

Over 24 h, sound levels were dominated by the highest levels within the recorded timespan. This means that the modeled, 24-h, 75th percentile sound level matches the recorded daily sound level more closely than the 50th percentile level. The average result skews toward the higher sound levels when sound levels are averaged over a longer timespan (e.g., over 24 h).

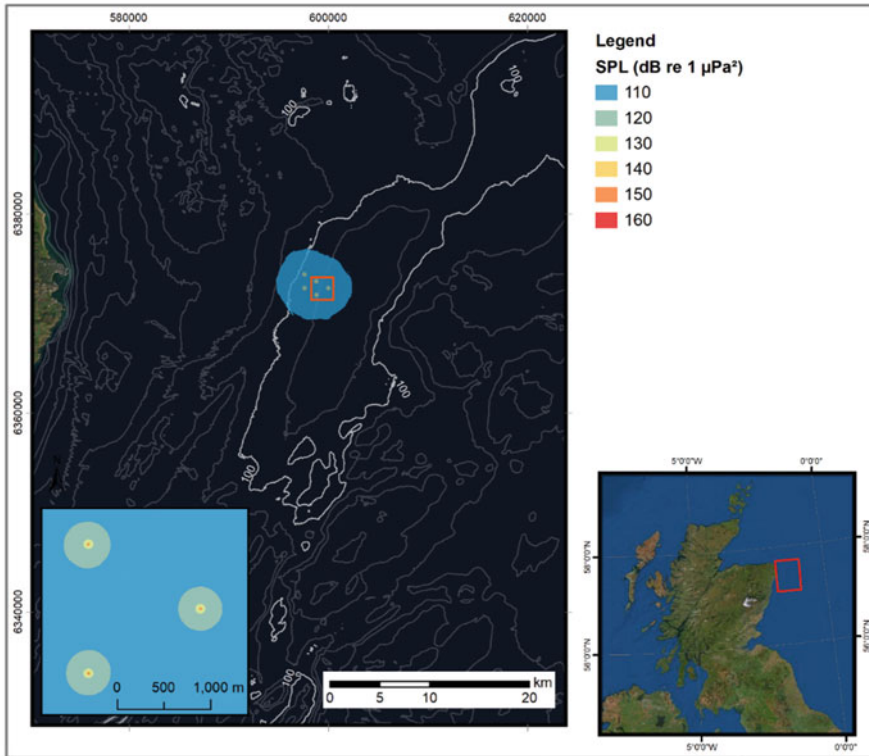


**Fig. 17** The radiated sound field modeled at the HYWIND site. The model assumed a 10-knot wind speed for the 50th percentile source levels. Datum WGS84 projection UTM30N

The maximum distances to the recommended TTS-onset sound levels for the auditory groups of interest (see Table 5) are those for receivers that are stationary for the exposure duration at the depth at which the sound level is at its loudest. The maximum distance to the TTS isopleth for the cases analyzed, when considering the 75th percentile, is for the very high-frequency cetacean hearing group at an 80-m maximum distance. Sound levels were highly variable, so the exact distances vary.

## Conclusions

The AMAR located at the HYWIND site was approximately equidistant from the three monitored turbines and it was situated to isolate HS-1 to the east. This set up allowed for an uncontaminated directional analysis of one HYWIND Scotland system.

A substantial contribution to the overall noise field from the wind farm was found to be constituted by several transient sounds thought to be associated with the mooring system. Despite the design of the mooring system being identical for

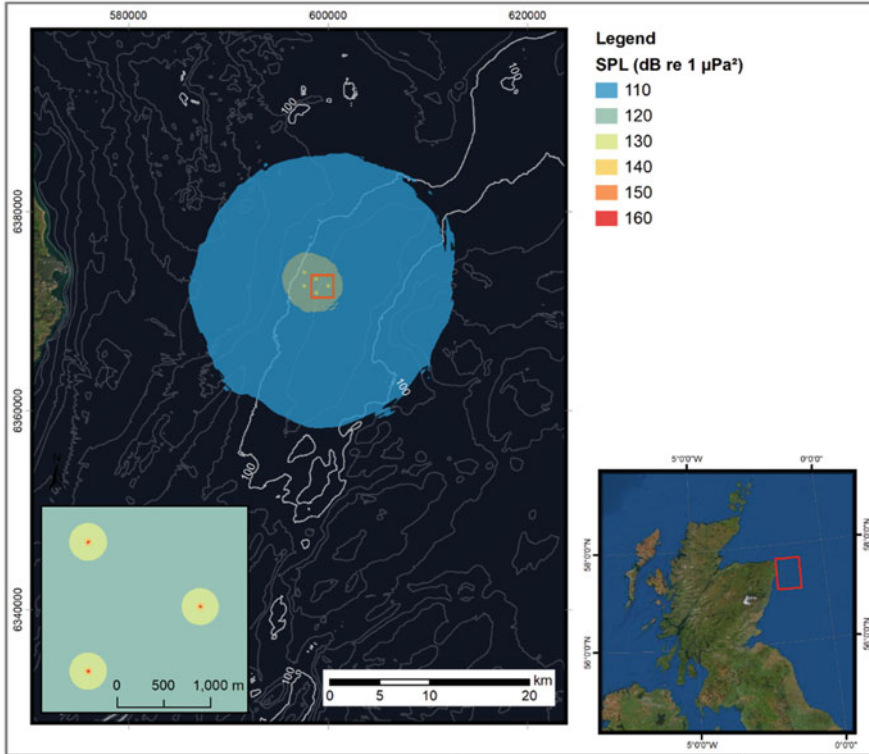


**Fig. 18** The radiated sound field modeled at the HYWIND site. The model assumed a 25-knot wind speed for the 95th percentile source levels. Datum WGS84 projection UTM30N

**Table 4** Modeled median and 75th percentile 24-h SEL ( $SEL_{24h}$ ; units:  $dB \text{ re } 1 \mu Pa^2 m^2 s$ ), assuming a wind speed of 15 knots. The auditory group frequency weightings are from Southall et al. (2019)

Auditory group	Auditory weighting function	Weighted received $SEL_{24h}$	
		50th percentile	75th percentile
Low-frequency cetaceans	LF	157.9	158.3
High-frequency cetaceans	HF	139.5	141.3
Very high-frequency cetaceans	VHF	137.2	138.8
Phocid carnivores in water	PCW	148.9	150.4
Other marine carnivores in water	OCW	148.8	150.5

each monitored turbine, unique signatures were identified for each of the three WTGs characterized. This means that it would be difficult to predict the characteristics of mooring sounds generated in a proposed wind farm installation during the impact assessment stage.

**Table 5** Modeled maximum distances (unit: m) to the temporary threshold shift (TTS; unit: dB re 1  $\mu\text{Pa}^2\text{s}$ ) threshold levels from Southall et al. (2019), assuming a wind speed of 15 kn

Auditory group	Auditory weighting function	TTS onset level	Maximum distance to weighted $\text{SEL}_{24\text{h}}$ TTS isopleth	
			50th percentile	75th percentile
Low-frequency cetaceans	LF	179	40	50
High-frequency cetaceans	HF	178	10	20
Very high-frequency cetaceans	VHF	153	50	80
Phocid carnivores in water	PCW	181	20	30
Other marine carnivores in water	OCW	199	<10	<10

Unlike the HYWIND demonstration system recordings from 2011, there was little evidence of highly impulsive, “snap” noises (Martin et al. 2011). However, there was a much great amount of transient noise from moorings. This mooring noise had distinct characteristics related to individual HYWIND systems. At HS-1, “bang” was produced, at HS-2 there was a “creak,” and at there was HS-4 a “rattle.” The directional processing of the AMAR array data showed that each type of sound was clearly connected with each system. Wave height positively correlated with occurrence. As wave height increased, there was a substantial corresponding increase in the contribution of the transient sounds to the overall sound signature of the wind farm.

A quantitative analysis of the impulsiveness of the HYWIND soundscape applied an impulse detector and studied the distribution of the per-minute kurtosis. Summing the SEL of all detected impulses showed that the impulsive SEL was generally less than 6 dB below the daily total SEL. The mean timespan of the impulses was  $\sim 1.5$  s, longer than the 1.0 s interval typically used to identify impulses to assess the effects of sound on hearing. The soundscape at the Control site had a lower kurtosis than at HYWIND; however, the kurtosis value for HYWIND was too low to be considered impulsive. Therefore, non-impulsive TTS SEL thresholds should be used to assess noise from wind farm.

The impulses per hour rate more positively correlated with wave height than with wind speed. A subjective aural analysis of these noises suggests a slightly lower rate of tension release in this particular mooring design; however, there is currently no quantifiable method with which to confirm this. Directional analysis of noise from the HS1, HS2, and HS4 moorings revealed that the noise came from mooring components at or from somewhere near the pillar itself. No available evidence suggests that the mooring noise was generated from the mooring system away from the bridle connection points on the HYWIND spar. This finding is reasonable since the most substantial movement in the mooring system likely occurs that at the

points where the chains are connected around the pillar because anchor chains fall through a ballasted catenary to the ocean floor and then sinks in the soil a distance away from the anchor. When analyzing mooring noise occurrence with wind speed only a limited correlation was found, but when comparing it with wave height a more direct relationship was identified. This result suggests that the dominant environmental factor influencing movement and associated mooring component friction in the floating structure is wave height.

The NMFS (2018) thresholds for temporary hearing thresholds shifts caused by non-impulsive sounds were applied to evaluate the possible effects on marine mammals by noise at HYWIND. The threshold for TTS was never exceeded and the daily marine mammal weighted SEL at both sites were very similar.

## References

- [ISO] International Organization for Standardization (2017) ISO/DIS 18405.2:2017. Underwater acoustics – terminology. Geneva. <https://www.iso.org/standard/62406.html>
- [NMFS] National Marine Fisheries Service (US) (2018) 2018 revision to: technical guidance for assessing the effects of anthropogenic sound on marine mammal hearing (version 2.0): underwater thresholds for onset of permanent and temporary threshold shifts. US Department of Commerce, NOAA. NOAA Technical Memorandum NMFS-OPR-59. 167 p. [https://media.fisheries.noaa.gov/dam-migration/tech\\_memo\\_acoustic\\_guidance\\_\(20\)\\_pdf\\_508.pdf](https://media.fisheries.noaa.gov/dam-migration/tech_memo_acoustic_guidance_(20)_pdf_508.pdf)
- Ainslie MA, Abrahamsen K, De Jong CAF, Delory E, Antonio-Díaz J, Ghasemi M, Lamaison V, Solheim Pettersen Ø, Slabbekoorn H et al (2021) SATURN acoustical terminology standard: draft. Document number 02466, version 1.0. Technical report by JASCO Applied Sciences for European Commission
- Austin ME, Chapman NR (2011) The use of tessellation in three-dimensional parabolic equation modeling. *J Comput Acoust* 19(3):221–239. <https://doi.org/10.1142/S0218396X11004328>
- Burns RDJ, Martin SB, Wood MA, Wilson CC, Lumsden CE, Pace F (2022) HYWIND Scotland floating offshore wind farm: sound source characterisation of operational floating turbines. Document number 02521, version 2.0. Technical report by JASCO Applied Sciences for Equinor Energy AS
- Collins MD (1998) New and improved parabolic equation models. *J Acoust Soc Am* 104(3): 1808–1808. <https://doi.org/10.1121/1.423601>
- Harrison CH, Harrison JA (1995) A simple relationship between frequency and range averages for broadband sonar. *J Acoust Soc Am* 97(2):1314–1317. <https://doi.org/10.1121/1.412172>
- Kaiser JF (1990) On a simple algorithm to calculate the ‘energy’ of a signal. In: IEEE international conference on acoustics, speech, and signal processing, Albuquerque, pp 381–384. <https://doi.org/10.1109/ICASSP.1990.115702>
- Kandia V, Stylianou Y (2006) Detection of sperm whale clicks based on the Teager-Kaiser energy operator. *Appl Acoust* 67:1144–1163. <https://doi.org/10.1016/j.apacoust.2006.05.007>
- Martin B, MacDonnell J, Vallarta J, Lumsden E, Burns RDJ (2011) HYWIND acoustics measurements report. Ambient levels and HYWIND Signature. Ver 1.3, Document number 00229. JASCO Applied Sciences (UK) Ltd. <https://static1.squarespace.com/static/52aa2773e4b0f29916f46675/t/5fda3a9324291a0a8b1d0a25/160813737245/Equinor-Hywind-Acoustic-Measurement-Report-JASCO-00229-December-2011.pdf>
- Martin SB, Lucke K, Barclay DR (2020) Techniques for distinguishing between impulsive and non-impulsive sound in the context of regulating sound exposure for marine mammals. *J Acoust Soc Am* 147(4):2159–2176. <https://doi.org/10.1121/10.0000971>
- Müller RAJ, Benda-Beckmann AMV, Halvorsen MB, Ainslie MA (2020) Application of kurtosis to underwater sound. *148(2):780–792*. <https://asa.scitation.org/doi/abs/10.1121/10.0001631>



- Pangerc T, Theobald PD, Wang LS, Robinson SP, Lepper PA (2016) Measurement and characterisation of radiated underwater sound from a 3.6. MW monopile wind turbine 140(4): 2913–2922. <https://asa.scitation.org/doi/abs/10.1121/1.4964824>
- Robinson SP, Lepper PA, Hazelwood RA (2014) Good practice guide for underwater noise measurement. In: National Measurement Office, Marine Scotland, and The Crown Estate (ed) NPL good practice guide no. 133. National Physical Laboratory, p 97
- Southall BL, Finneran JJ, Reichmuth CJ, Nachtigall PE, Ketten DR, Bowles AE, Ellison WT, Nowacek DP, Tyack PL (2019) Marine mammal noise exposure criteria: updated scientific recommendations for residual hearing effects. *Aquat Mamm* 45(2):125–232. <https://doi.org/10.1578/AM.45.2.2019.125>
- Stöber U, Thomsen F (2021) How could operational underwater sound from future offshore wind turbines impact marine life? *J Acoust Soc Am* 149(3):1791–1795. <https://doi.org/10.1121/10.0003760>
- Tougaard J, Hermannsen L, Madsen P (2020) How loud is the underwater noise from operating offshore wind turbines? *J Acoust Soc Am* 148:2885–2893
- Zhao Y-M, Qiu W, Zeng L, Chen S-S, Cheng X-R, Davis RI, Hamernik RP (2010) Application of the kurtosis statistic to the evaluation of the risk of hearing loss in workers exposed to high-level complex noise. *Ear Hear* 31(4):527–532. <https://doi.org/10.1097/AUD.0b013e3181d94e68>